Supplementary Information

SERS-based assay for multiplexed detection of cross-reactivity and persistence of antibodies against the spike of the native, P.1 and B.1.617.2 SARS-CoV-2 in non-hospitalised adults

Malama Chisanga[a], Matthew Stuible[b], Christian Gervais[b], Denis L'Abbé[b], Brian Cass[b], Louis Bisson[b], Alex Pelletier[b], Simon Lord-Dufour[b], Yves Durocher[b], Denis Boudreau[c], Sylvie Trottier[d], Joelle N. Pelletier[e†], Jean-Francois Masson[a†]

[a]Department of Chemistry, Quebec Centre for Advanced Materials (QCAM), Regroupement Québécois sur les Matériaux de Pointe (RQMP), and Centre interdisciplinaire de recherche sur le cerveau et l'apprentissage (CIRCA), Université de Montréal, CP 6128 Succ. Centre-Ville, Montreal, Québec, H3C 3J7, Canada.
[b]Mammalian Cell Expression, Human Health Therapeutics Research Centre, National Research Council Canada, Montréal, QC, Canada.
[c]Department of Chemistry and Centre for Optics, Photonics and Lasers (COPL), Université Laval, 1045, av. de la Médecine, Québec, QC G1V 0A6, Canada.
[d]Centre de recherche du Centre hospitalier universitaire de Québec and Département de microbiologie-infectiologie et d'immunologie, Université Laval 2705, boulevard Laurier, Québec, QC, Canada G1V 4G2
[e]Department of Chemistry, Department of Biochemistry and PROTEO, Québec Network for Research on Protein Function, Engineering and Applications, Université de Montréal, CP 6128 Succ. Centre-Ville, Montreal, Québec, H3C 3J7, Canada.

[†]Corresponding authors

Joëlle Pelletier: E-mail: joelle.pelletier@umontreal.ca, Tel: +1-514-343-2124

Jean-Francois Masson: E-mail: jf.masson@umontreal.ca, Tel: +1-514-343-7342

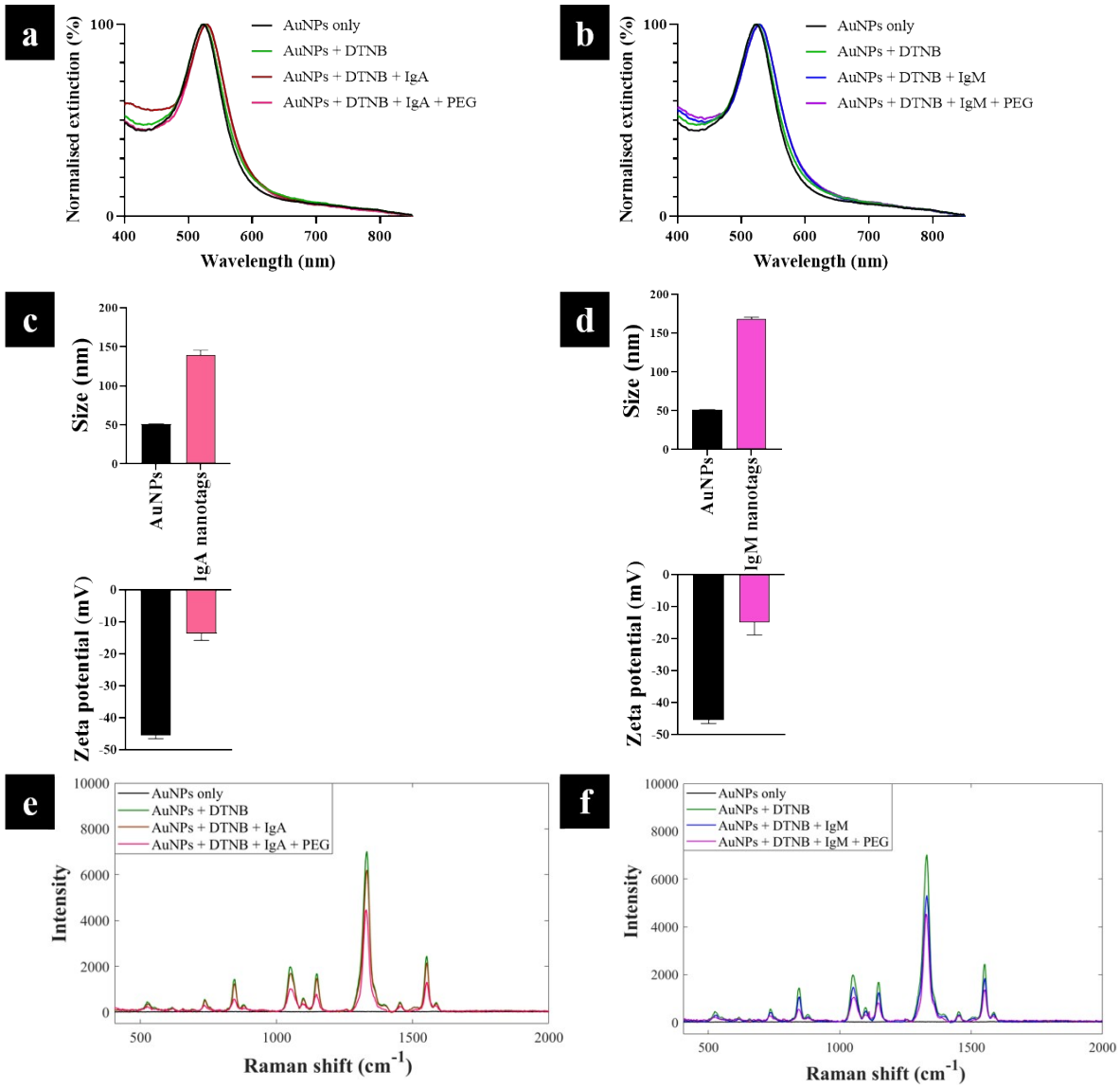

Figure S1. Characterisation steps of the SERS-active biorecognition nanosensors before and after functionalisation of AuNPs: **(a, b)** Redshifting UV-vis extinction spectra, **(c, d)** increased dynamic light scattering and reduced zeta potential readings, and corresponding intense SERS spectra **(e, f)** detected for anti-spike IgA and IgM antibodies, respectively. Error bars on **(c, d)** represent one standard deviation of the mean from triplicate measurements.

The extinction spectral data in Figure S1a-b show plasmonic bands of AuNPs before and after surface conjugation for IgA and IgM nanotags. The λ_{max} of bare AuNPs colloid detected at 530 nm, the λ_{max} of IgG functionalised nanotags displayed clear shift to higher walengths of Δ7 nm and Δ8 nm for IgA and IgM nanotags, respectively as a result of changes in the refractive index of suspensions on successful conjugation. Similar to IgG nanotags seen in Figure 1, IgA and IgM tags retained single symmetrical LSPR in the 350–800 nm wavelength range, which was indicative of isotropic, monodispersed and stable conjugates. IgA and IgM conjugation onto particles surface was further confirmed by increase in hydrodynamic diameters (D_H) from 51 ± 0.3 nm to 139 ± 6.5 nm and 51 ± 0.3 to 168 ± 2.4 nm and corresponding decrease in zeta potential from -45 ± 1.1 mV to -14 ± 2.1 mV and -45 ± 1.1 to -15 ± 3.8 nm for IgA and IgM capture antibodies, respectively. These readings reflected the changes in particle density, size and surface environment after conjugating DTNB, antibodies and PEG to AuNPs (Figure S1c-d). The SERS data measured from the nanosensors showed slight decreases in band intensities for both IgA and IgM nanotags compared to AuNP-reporter conjugates as shown in Figure S1e-f . However, the decrease in band intensities did not appear to significantly affect detection sensitivity of recognition nanotags.

Determination of antibody coverage

The Bradford protein assay was used to quantify antibodies present in each sample, and to calculate the number of antibody molecules/Au nanosphere. Calibration curves were plotted from serial dilutions prepared from 60 µg/mL of standard antibody stock solutions.

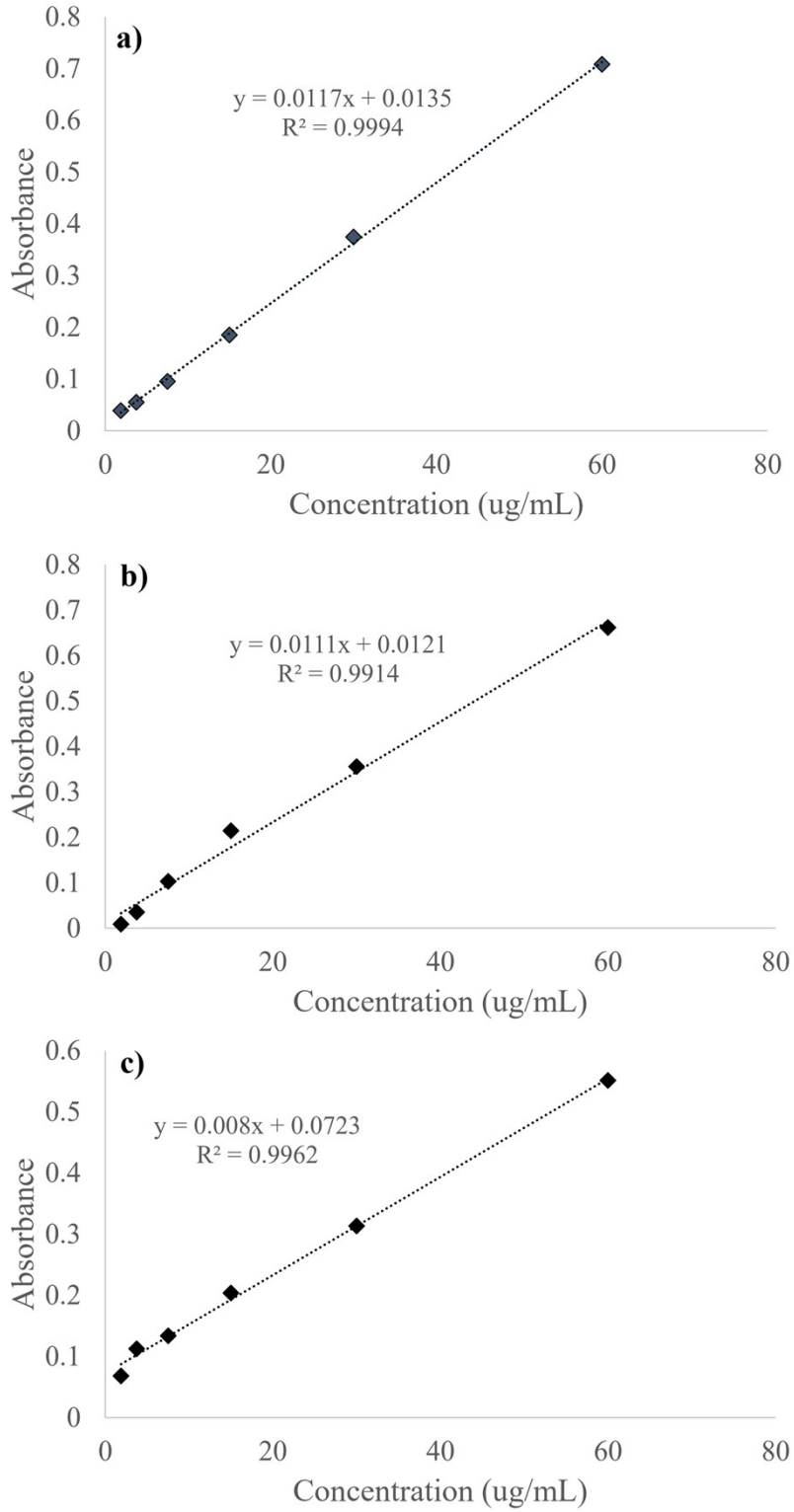

Figure S2. Bradford protein assay calibration curve for **(a)** IgG, **(b)** IgA and **(c)** IgM standard antibodies used to determine the concentration of capture antibodies adsorbed onto nanoparticles. The number of antibodies/AuNP were estimated to be 60, 42, 33 for IgG, IgA and IgM antibodies, respectively.

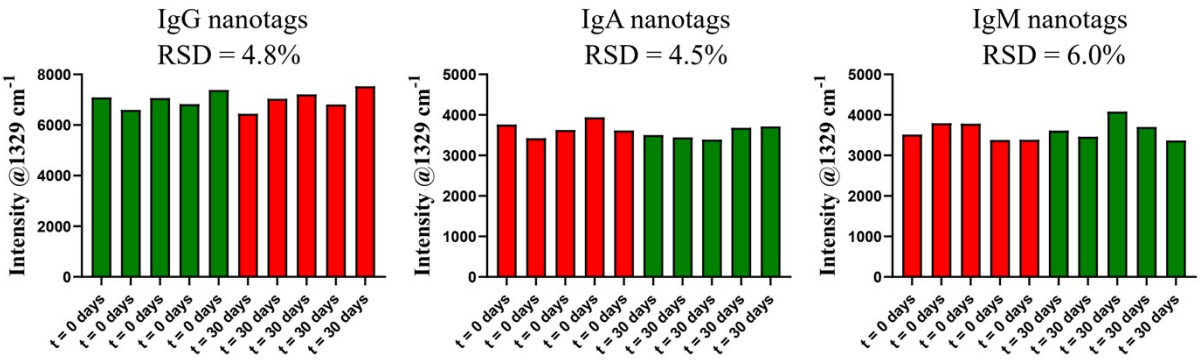

Figure S3. Time-course assessment of stability and reproducibility of nanotags synthesised via passive binding strategy. The nanotags were tested in a pooled serum on different days from the first day of synthesis (t = 0 days, green bars) to the final day (t = 30 days, red bars) using five repeat measurements at each time point. Here, we demonstrate that the nanotags were highly stable and reproducible as highlighted by very low relative standard deviation (RSD) of ≤6%, indicative of well-performing SERS nanotags.[1]

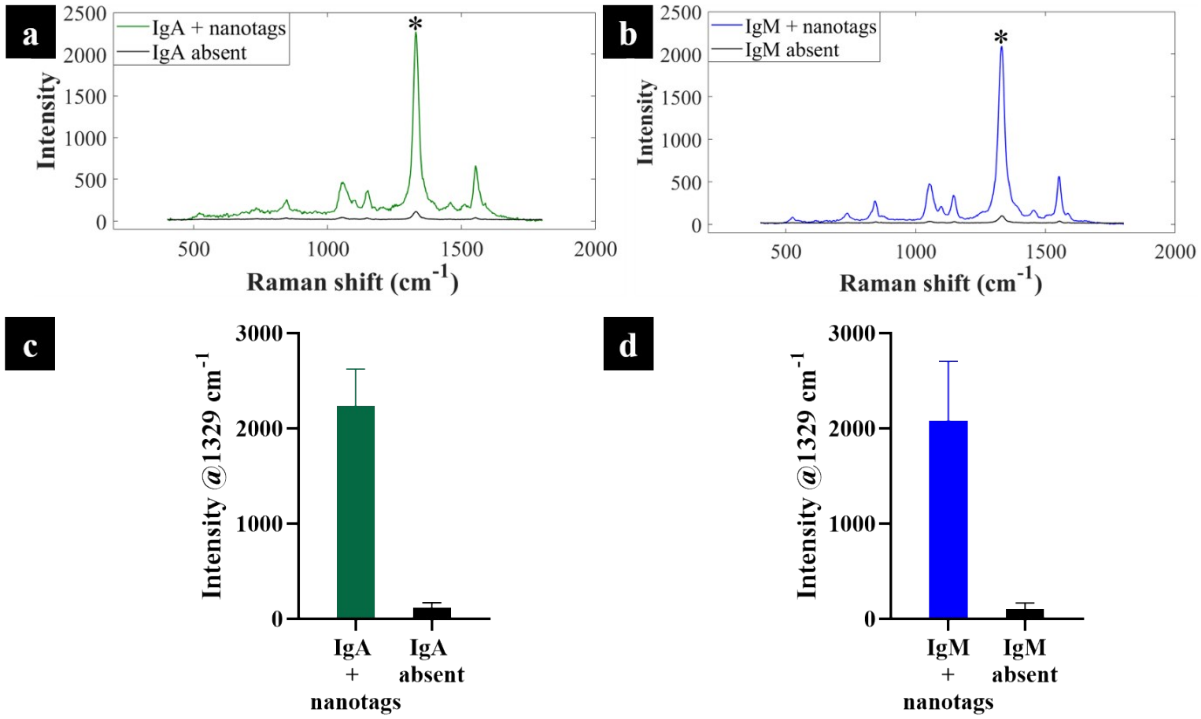

Figure S4. Principle of the microfluidic-integrated multiplexed SERS assay employing anti-human IgA and IgM recognition nanotags to detect sera antibodies binding to the native spike protein. SERS signals **(a)** yielded and corresponding bar intensity plots **(c)** when IgA-spike complexes are present (green trace) and when IgA-spike is absent (black trace). SERS spectra **(b)** observed and corresponding bar graph intensity plots **(d)** representing when IgM-spike conjugates are present (blue trace) and when the IgM-spike is absent (black trace). Asterisks (*) indicate the SERS marker band used to identify the Raman reporter (DTNB) and measure multiple antibody-spike interactions and cross-reactivities in spatially separated microfluidic channels.

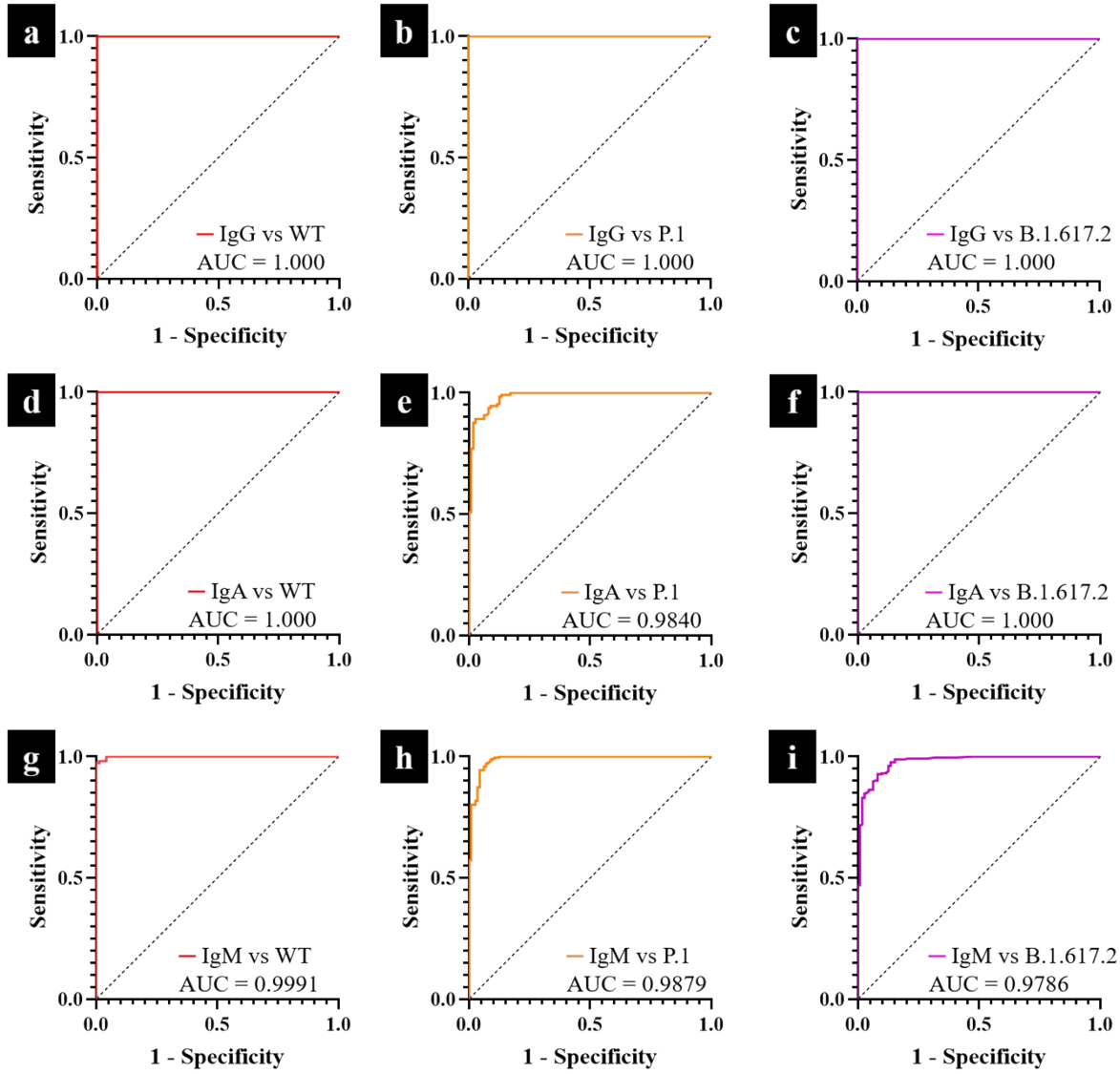

Figure S5. ROC curves demonstrating high diagnostic performance of microfluidics-integrated multiplexed SERS assay used for observing multiple anti-spike antibody titres and cross-reactions simultaneously in previously PCR-positive to SARS-CoV-2 non-hospitalised seropositive individuals (n = 24) and seronegative adults (n = 8) for: **(a-c)** IgG-spike, **(d-f)** IgA-spike, and **(g-i)** IgM-spike at 3 weeks post-infection. WT: native strain. Decision thresholds were calculated as: mean + 3σ, where the mean and standard deviation (σ) are computed from negative controls. Area under the curve is (AUC) included on the figures.

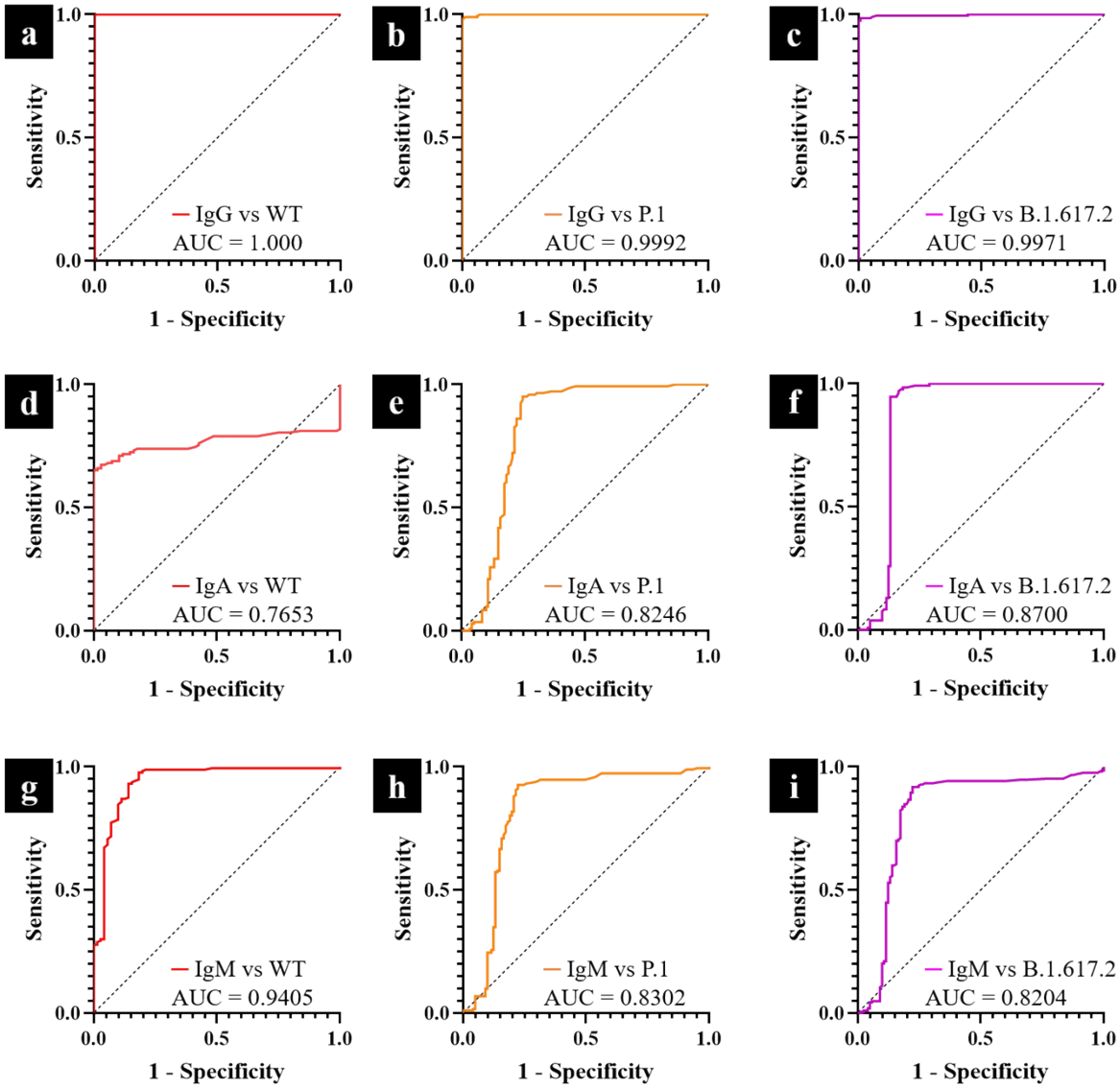

Figure S6. ROC curves demonstrating diagnostic performance of our microfluidics-integrated multiplexed SERS assay used to detect multiple anti-spike antibody responses and cross-reactions in seropositive previously PCR-positive to SARS-CoV-2 non-hospitalised adults (n = 24) compared with seronegative adults (n = 8) for: **(a-c)** IgG-spike, **(d-f)** IgA-spike, and **(g-i)** IgM-spike at 8 weeks post-symptom onset. WT: native strain. The decision thresholds were calculated as: mean + 3σ, where the mean and standard deviations (σ) were determined from negative controls. Area under the curve is (AUC) included on each figure.

It can be seen that when sera samples were collected by 8 weeks after COVID-19 diagnosis, sensitivity and specificity for IgG against the native spike protein was high (AUC: 1.000), compared to that for IgA (sensitivity 66%, specificity 97%) and lastly IgM (sensitivity 43%, specificity 96%) antibodies. Similarly, strongest antibody-spike antibody responses and cross-reactions were observed for IgG leading to high detection accuracy against the P.1 spike (sensitivity 98%, specificity 100%) and the B.1.617.2 spike (sensitivity 98%, specificity >99%), followed by IgA against the P.1 spike protein (sensitivity >13%, specificity >89%) and the B.1.617.2 spike (sensitivity >13%, specificity >89%). The ability of convalescent sera IgM to offer cross-protection against the VOCs declined considerably, and this led to much lower detection accuracy against the P.1 spike (sensitivity >24%, specificity >90%) and the B.1.617.2 spike protein (seropositivity >32%, seronegativity >88%) after 8 weeks post onset of COVID-19 symptoms. Overall, the sensitivity for IgG detection were highly robust, and this corroborate high levels of antibody responses detected at the same sampling time intervals illustrated on Figures 4 and 5 of the main article.

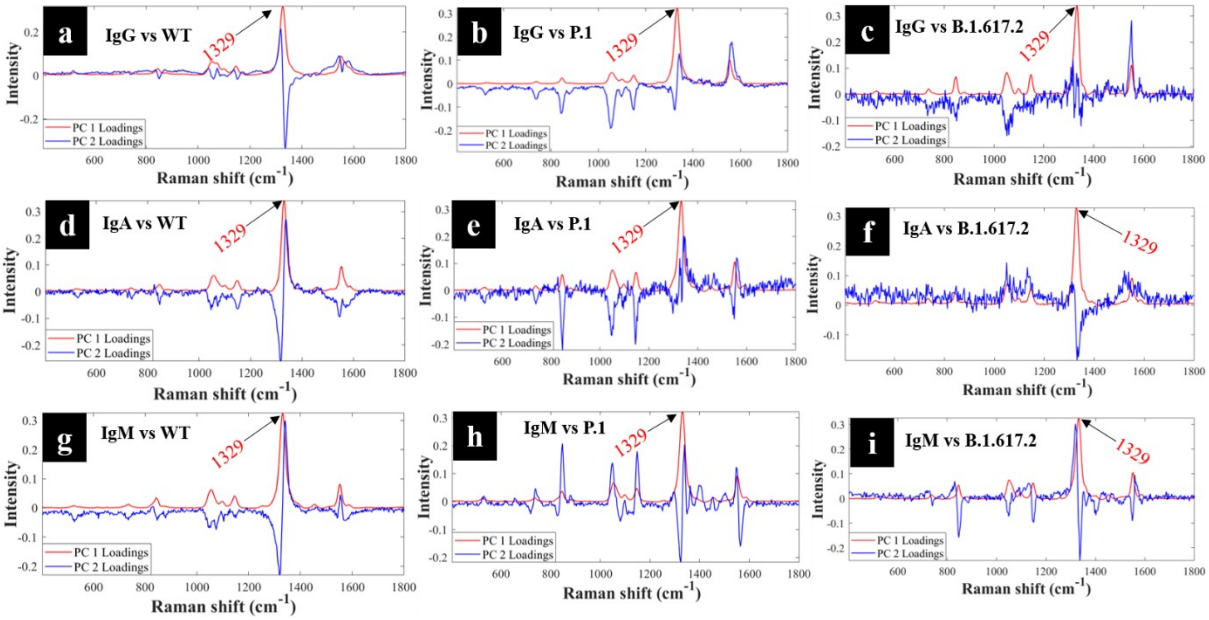

Figure S7. PC loadings for SERS assay spectral data of multiple anti-spike antibody titres simultaneously detected in clinical samples: **(a-c)** IgG-spike, **(d-f)** IgA-spike, and **(g-i)** IgM-spike interactions. The numbers (red) and arrowheads on respective spectral peaks represent wavenumbers of the major explanatory input variables associated with clustering patterns seen on the PCA (**Figure 6**) of the main article. WT: native strain. Specific antibody-spike interactions are annotated accordingly on each figure with columns representing antibody-native, antibody-P.1 and antibody-B.1.617.2 spike interactions from left to right.

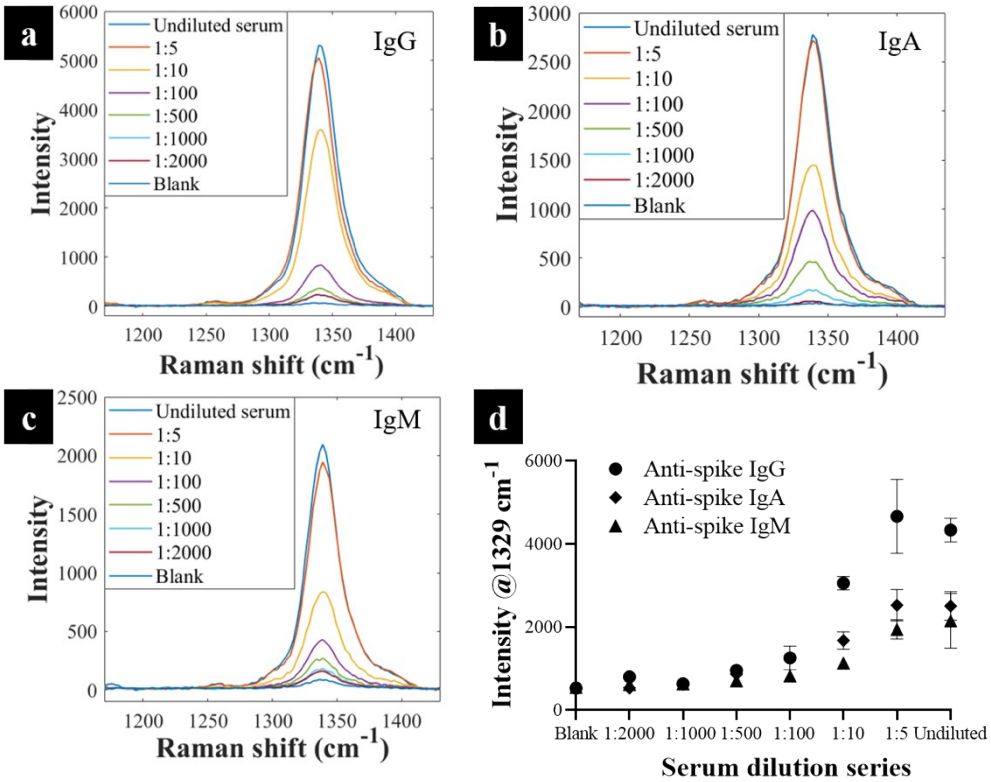

Figure S8. Quantitative assessment of SERS spectral signals measured from antibody-spike secondary immunoreactions from which binding affinities (K_Ds) were calculated for spike-specific **(a)** IgG, **(b)** IgA, and **(c)** IgM. **(d)** Corresponding calibration curves of antibodies plotted from quantitative spectral data presented in **a-c**. Error bars on **(d)** represent one standard deviation.

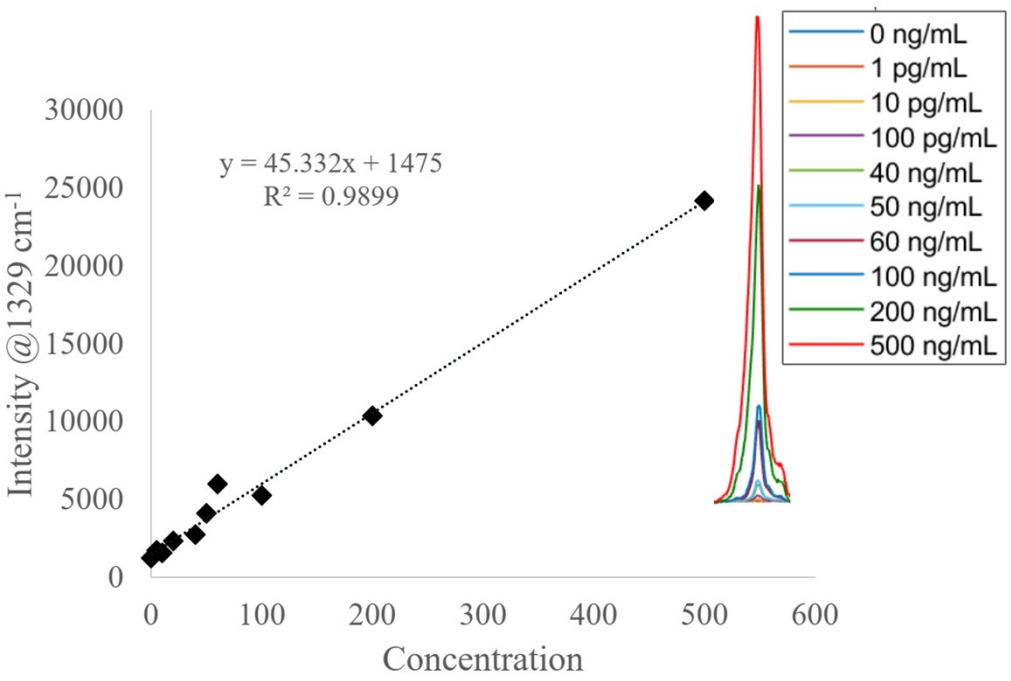

Figure 9. Quantitative analysis of primary human IgG antibody using microfluidics-integrated SERS assay developed in this study. The limit of detection (LOD) of our SERS assay was 5 pg/mL, which is orders of magnitude better than that reported for standard clinical assays such as ELISA and LFIA.

References

1. D. B. Grys, R. Chikkaraddy, M. Kamp, O. A. Scherman, J. J. Baumberg and B. de Nijs, *J. Raman Spectrosc.*, 2021, **52**, 412-419.